

# The X-ray properties of the nearby LINER galaxy, NGC 4736

T. P. Roberts<sup>1</sup>, R. S. Warwick<sup>1</sup> & T. Ohashi<sup>2</sup>

<sup>1</sup>*Department of Physics and Astronomy, University of Leicester, University Road, Leicester, LE1 7RH*

<sup>2</sup>*Department of Physics, School of Science, Tokyo Metropolitan University, 1-1 Minami-Ohsawa, Hachioji, Tokyo 192-03*

## ABSTRACT

NGC 4736 is a nearby Sab spiral galaxy, hosting one of the closest examples of a LINER nucleus. We have utilized recent observations by *ROSAT* and *ASCA* to characterise the X-ray properties of this galaxy. Twelve discrete X-ray sources are detected within the region subtended by its optical disk, the majority of which are likely to be X-ray binaries associated with the galaxy. By far the brightest source in the X-ray band is positionally coincident with the nucleus of the galaxy and is spatially resolved into a component with a radial extent of  $\sim 3$  kpc plus a point-like core. The broad band (0.1–10 keV) spectrum of this nuclear source is composed of a hard continuum with a spectral slope characteristic of that observed in classical Seyfert nuclei (*i.e.* power-law photon index,  $\Gamma \approx 1.7$ ), with thermal emission ( $kT = 0.1 - 0.6$  keV) dominant below 2 keV. An Fe  $K_{\alpha}$  line may also be present at  $\sim 6.8$  keV. There is no evidence for X-ray temporal variability on timescales of hours to years. A plausible model is that the hard continuum originates in a near-quiet active galactic nucleus (with  $L_X \sim 6 \times 10^{39}$  erg s<sup>-1</sup>, 0.5–10 keV) embedded in the LINER at the centre of NGC 4736. However, an alternative explanation, namely that the LINER is the site of a dense population of X-ray binary sources, cannot be completely excluded.

**Key words:** galaxies:individual:NGC 4736 – galaxies:nuclei – X-rays:galaxies.

## 1 INTRODUCTION

NGC 4736 (Messier 94) is a nearby, face-on spiral galaxy of morphological type Sab, located in a sub-group of the Coma-Sculptor cloud of galaxies at a distance of 4.3 Mpc (Tully 1988). Studies over a range of wavebands have helped define the distinctive morphological properties of this galaxy. For example, using optical and H I observations Bosma, van der Hulst & Sullivan (1977) identify five separate annular regions namely (i) a bright central region (the bulge), within a radius,  $R < 15''$ ; (ii) an inner spiral structure,  $R \sim 15'' - 50''$ , which is bounded by a bright inner ring; (iii) an outer spiral structure,  $R \sim 50'' - 200''$ , forming an outer disc; (iv) a zone of low surface brightness and (v) a faint outer ring at  $R \sim 330''$ .

Buta (1988) first identified the bright inner ring as a circumnuclear star-formation region. In the H $\alpha$  observations of Pogge (1989), the ring appears oval with a slight extension along the south-east to north-west axis, and to be clumpy in nature. The ring structure is also prominent in H I (Mulder & van Driel 1993), in molecular gas (Gerin, Casoli & Combes 1991) and in the far infrared (Smith et al. 1991). Further evidence for an active environment comes from the 6 cm radio continuum observations of Turner & Ho (1994), who observe

a series of non-thermal emission sources coincident with the ring which are probably associated with recent supernovae (RSN) or supernova remnants (SNR).

The morphology of the bright central region of NGC 4736 has been studied in detail using surface photometry in the visual, NIR and H $\alpha$  bands by Möllenhoff, Matthias & Gerhard (1995), who found evidence for a weak nuclear bar of size  $\approx 30'' \times 9''$  aligned roughly along a north-south axis. However, most studies of the nucleus have focussed on spectroscopic data which reveal the presence of a low-ionisation nuclear emission-line region (LINER, Heckman, Balick & Crane 1980). Here the debate centres on whether the emission line spectrum is powered by a low-luminosity active galactic nucleus (LLAGN) or is the result of shock excitation and/or photoionisation from young, hot stars. Filippenko & Sargent (1985) re-classified the source as a *Transition* LINER since the low-ionisation nuclear emission lines are interspersed with emission lines characteristic of star-formation. This is confirmed by the study of Larkin et al. (1998), who investigated the near-infrared spectra of a sample of LINER galaxies, and found NGC 4736 to show the strongest FeII/Pa $\beta$  line ratio of any of their sample, suggesting that, at least in this waveband, star-

formation is the dominant process. In fact, the presence of a LLAGN in NGC 4736 is called into question on the basis of several observations. Most particularly, the absorption-corrected  $H\alpha$  luminosity in the central ( $37 \text{ pc} \times 60 \text{ pc}$ ) region of the nucleus may be accounted for by the presence of just six O6 stars (Taniguchi et al. 1996). Also, the far-infrared emission, which is peaked at the position of the nucleus, may be powered solely by the emission of non-OB stars (Smith et al. 1991; Smith et al. 1994), and excludes the presence of an AGN unless the absorption of the nucleus was underestimated by the authors. Thus it has been suggested by Taniguchi et al. (1996) that NGC 4736 is a “post-starburst” galactic nucleus, an example of a LINER created in the absence of AGN activity.

Despite the arguments cited above, a LLAGN may still exist at the heart of NGC 4736. For example, Turner & Ho (1994) have observed a strong non-thermal radio continuum source at the position of the nucleus, which they identify as an AGN candidate. Also, in the recent survey of nearby galactic nuclei of Ho, Filippenko & Sargent (1997), the central  $40 \text{ pc} \times 80 \text{ pc}$  region of the nucleus is classified as a *pure* LINER region, which again has been taken as evidence for an AGN (Ho, Filippenko & Sargent 1998). More compellingly, *Hubble Space Telescope* UV observations of the nucleus of NGC 4736 (Maoz et al. 1995) reveal a bright point source surrounded by diffuse emission at the exact optical nucleus position. This source is seen to have a point-like companion source of equal brightness at a distance of  $2.5''$  ( $\sim 50 \text{ pc}$ ) directly north of the first source. Although both sources may be compact star clusters, an alternative possibility is that NGC 4736 contains not one but *two* supermassive black holes that are in the process of merging. This idea is discussed by Taniguchi & Wada (1996), who model the effect of a galaxy merger between a main galaxy and a nucleated satellite galaxy. Such a merger may create a supermassive black hole binary in the nucleus of the main galaxy, which can trigger a starburst and bow shocks consistent with what is seen in NGC 4736. A galaxy merger may also create the ring structure seen in NGC 4736, the most famous example of such an event being the “Cartwheel” galaxy (Struck et al. 1996). In this scenario, the weak LINER spectrum and low  $H\alpha$  and far-infrared emission in the nucleus may then be explained by the post-starburst nucleus containing a LLAGN in a relatively quiescent state.

One way of progressing the debate concerning the origin of the LINER in NGC 4736 is to consider the X-ray properties of the source. The most detailed study of NGC 4736 in the high energy band is that reported by Cui, Feldkhun & Braun (1997) who have analysed a deep pointed observation carried out with the *ROSAT* X-ray Telescope/Position Sensitive Proportional Counter (PSPC). They found evidence for an extended distribution of hot ( $kT \approx 0.3 \text{ keV}$ ) gas within the central few kiloparsec region of NGC 4736, in addition to a compact, relative low luminosity ( $L_X \approx 3 \times 10^{39} \text{ erg s}^{-1}$ ,  $0.1 - 2 \text{ keV}$ ) nuclear X-ray source. Clearly, a plausible interpretation is that this compact X-ray source corresponds to a LLAGN, although other explanations are possible. Cui et al. (1997) also report the detection of a further point-like source offset by  $\sim 1'$  from the compact nuclear source, which is perhaps best explained as a bright X-ray transient in NGC 4736.

Subsequent to the PSPC observation NGC 4736 has

been the subject of further study in the X-ray regime. Specifically it has been observed on two occasions with the *ROSAT* High Resolution Imager (HRI) and also once by *ASCA*. In this paper we utilize all the available datasets from *ROSAT* and *ASCA* to further investigate both the discrete X-ray source population in NGC 4736 and the nature of its central X-ray source. The next section briefly describes the set of observations and the techniques we have employed to reduce the data. Section 3 then focusses on the discrete X-ray sources detected in the various *ROSAT* images of NGC 4736, whereas in section 4 we present the results pertaining to the spatial, spectral and temporal properties of its nuclear emission. Finally in section 5 we return to the question of whether the LINER nucleus of NGC 4736 harbours a LLAGN or is powered entirely by star-formation processes.

## 2 OBSERVATIONS AND DATA REDUCTION

Details of the *ROSAT* and *ASCA* observations of NGC 4736 used in the present paper are given in Table 1. The preliminary processing of the *ROSAT* PSPC data involved excluding time intervals when the charged-particle master-veto rate was in excess of  $170 \text{ count s}^{-1}$ . This resulted in the rejection of 11% of the raw data, leaving  $\sim 85 \text{ ks}$  of “clean” data. For the spatial and temporal analysis the PSPC data were divided into a soft band (corresponding to PI channels 11–41 and energy range  $0.1\text{--}0.4 \text{ keV}$ ) and a hard band (PI channels 52–200 and energy range  $0.5\text{--}2 \text{ keV}$ ). Preliminary images in both bands were produced on a  $15'' \times 15''$  spatial grid.

Two separate *ROSAT* HRI observations of NGC 4736 have been performed (Table 1); hereafter we refer to the first (and deeper) observation as HRIa and the second as HRIb. Preliminary HRI images were produced using data from PI channels 3 – 8 and a  $8'' \times 8''$  pixel grid.

The *ASCA* data were screened using standard procedures (via the FTOOLS package), leading to a total of  $\sim 27 \text{ ks}$  of “clean” data from each of the SIS and GIS instruments. Since the spatial resolution of the *ASCA* X-ray telescope is relatively poor, compared to that of the *ROSAT* X-ray telescope, the analysis of the *ASCA* observations concentrated on the spectral and temporal characteristics of the source.

X-ray spectra of the bright central X-ray source in NGC 4736 (see section 3) were obtained from the *ROSAT* PSPC and from the *ASCA* SIS and GIS instruments. The PSPC spectrum was extracted using a circular aperture of radius of  $2'$  centred on the galaxy nucleus. The resulting pulse-height data were background subtracted (using data from a source free-region in the *ROSAT* PSPC field) and vignetting corrected and then rebinned into  $\sim 30$  spectral channels encompassing the full  $0.1\text{--}2.4 \text{ keV}$  bandpass of the PSPC. In the case of *ASCA*, the REV2 standard datasets were used to take advantage of the most recent *ASCA* calibration files. The source spectra were derived from a  $3'$  radius region centred on NGC 4736 with the background data taken from the same observation. The spectral binning was based on the requirement of a minimum of 20 counts per bin within a spectral range of  $0.6\text{--}10 \text{ keV}$  and  $0.8\text{--}10 \text{ keV}$  for the SIS and GIS instruments respectively.

**Table 1.** Details of the *ROSAT* and *ASCA* observations of NGC 4736

Satellite/ instrument(s)	Observation identification	Pointing direction		Exposure (s)	Start date (year.day)
		RA(2000)	Dec(2000)		
<i>ROSAT</i> PSPC	rp600050n00	12 <sup>h</sup> 50 <sup>m</sup> 50.3 <sup>s</sup>	41°06′35″	94819	91.156
<i>ROSAT</i> HRI	rh600678n00	12 <sup>h</sup> 50 <sup>m</sup> 52.7 <sup>s</sup>	41°07′11″	112910	94.341
<i>ROSAT</i> HRI	rh600769n00	12 <sup>h</sup> 50 <sup>m</sup> 52.7 <sup>s</sup>	41°07′11″	27292	94.359
<i>ASCA</i> SIS + GIS	63020000	12 <sup>h</sup> 50 <sup>m</sup> 53.0 <sup>s</sup>	41°07′15″	40000	95.145

### 3 DISCRETE X-RAY SOURCES ASSOCIATED WITH NGC 4736

The central regions of the *ROSAT* PSPC and HRI images were searched for discrete X-ray sources using the PSS software which is part of the Starlink ASTERIX package (Allan 1995). Those sources detected in the *ROSAT* observations with a significance  $\geq 5\sigma$  by the PSS algorithm and lying within a  $12' \times 12'$  field centred on NGC 4736 are listed in Table 2, with a source designation of the form “N4736-X $i$ ”. The table also gives for each source the position and position error (derived preferentially from the HRI data) and the measured count rate in the soft and hard PSPC bands and both HRI observations (with a dash signifying a non-detection at the  $5\sigma$  threshold). A total of 15 discrete sources were detected, 12 of which lie within the elliptical region defined by a major axis dimension ( $D_{25}$  diameter) of 11.8' and an axial ratio  $b/a = 0.87$  (Tully 1988). Figure 1 shows the optical image of the galaxy taken from the Palomar Digitised Sky Survey (DSS) with the  $D_{25}$  ellipse and the positions of the X-ray sources overlaid. The low-surface brightness gap and the faint outer ring described by Bosma, van der Hulst & Sullivan (1977) are clearly visible in the DSS image; unfortunately the high surface brightness of the three inner zones renders these regions indistinguishable. The last column of Table 2 notes possible bright optical counterparts to the X-ray sources (as discernable in Figure 1) and also whether the source is positionally coincident with either the optical disc (OD) or the faint outer-ring (OR) of the galaxy.

Inspection of Table 2 shows that the brightest discrete X-ray source in NGC 4736 has a count rate at least a factor 30 larger than any other source and, within the measurement errors, is positionally coincident with the optical nucleus of the galaxy. This “nuclear” X-ray source is partially resolved in both the *ROSAT* PSPC and HRI observations and is discussed in the next section. None of the other sources are bright enough for a detailed X-ray spectral or temporal analysis to be carried out. However, it is possible to comment on the possible nature of some of the sources. For example, N4736-X2 is the only source, other than the nuclear source, to be detected in both the PSPC soft and hard bands and also in both HRI observations. This source lies in the outer ring of NGC 4736 and is 24" north of what appears to be a bright foreground star. However, for this star to be the source of the X-rays requires either that it has a large proper motion or that the X-ray positions suffer from an aspect error (in the form of a rotation). We consider neither of these a likely scenario. Two further discrete sources spatially coincident with the outer ring of NGC 4736 (N4736-X11 and N4736-X15) are detected only in the soft PSPC band. These may be “Super-Soft Sources” (SSS; see Singh et al. 1995 and references therein), a rare type of object with a black-body continuum spectrum of temperature of  $\sim 30$  eV and lumi-

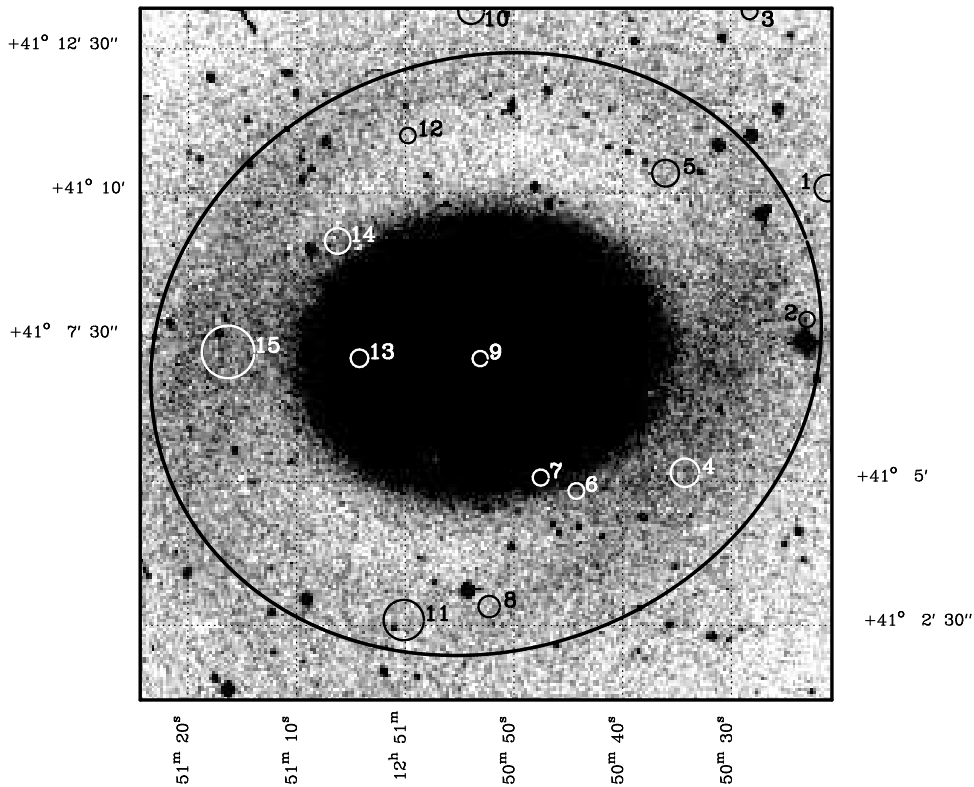
nosity  $\lesssim 10^{38}$  erg s $^{-1}$ , thought to contain an accreting white dwarf (van den Heuval et al. 1992). In fact, if these sources are at the distance of NGC 4736 and absorbed only by the foreground Galactic column ( $N_H = 1.4 \times 10^{20}$  cm $^{-2}$ ) then their observed luminosities are of the order  $7 \times 10^{36}$  erg s $^{-1}$  in the 0.1–0.4 keV band, which is not inconsistent with the SSS hypothesis. However, the presence of a bright optical object in the error box of N4736-X11 suggests two further possibilities, namely that this source is either a foreground object (such as a magnetic CV or white dwarf) or an ultra-soft background object (such as a narrow-line Seyfert I; see Brandt, Pounds & Fink 1995).

Of course, a number of the sources located in the field of NGC 4736 may not be physically associated with the galaxy. For example, the deep PSPC observation reaches down to a flux threshold of  $5 \times 10^{-15}$  erg cm $^{-2}$  s $^{-1}$  and using the corrected 0.5–2 keV  $\log N - \log S$  derived by Hasinger et al. (1994), we estimate the source density at this limit to be  $\sim 200$  sources per square degree, or  $\sim 5$  sources within the  $D_{25}$  ellipse of NGC 4736. This is to be compared to the 11 sources observed (excluding the nuclear source). However, this argument does ignore the obscuration due to the H I associated with the disc of NGC 4736, an effect which could substantially reduce the incidence of “serendipitous” background sources. Even if we assume that the bulk of the sources in the field are associated with NGC 4736, then the implied number of  $L_X \sim 10^{37}$  erg s $^{-1}$  sources associated with this galaxy does not look particularly untoward for a bright Sab spiral (*c.f.* Read, Ponman & Strickland 1997).

Using the measured hard band PSPC and HRI count rates we can search for long term variability provided we assume the sources are all point-like, (*i.e.* not partially resolved by the HRI) and have a specific spectral form. Hypothesising that in the 0.5–2 keV energy range the brightest population of sources in NGC 4736 would be X-ray binary systems (XRBs), then a reasonable assumption is a thermal bremsstrahlung spectrum with a mean temperature  $kT \approx 1.8$  keV (Read, Ponman & Strickland 1997). We also assume a line of sight absorption of  $3 \times 10^{20}$  atoms cm $^{-2}$ , that is roughly twice Galactic  $N_H$  so as to make some allowance for any absorption intrinsic to NGC 4736. On this basis, of the 8 sources investigated, only two show significant variability between the observations. Source N4736-X6 is more than 3 times more luminous in observation HRIa than in the PSPC observation made 3.5 years earlier (based on an upper limit to the flux in the latter measurement). Similarly, N4736-X12 exhibited a factor  $\gtrsim 9$  increase between the PSPC and the HRIb observations (a factor  $\gtrsim 3$  change in 18 days is also implied by the non-detection of this source in the HRIa observation).

**Table 2.** Discrete X-ray sources discovered within a  $12' \times 12'$  field centred on NGC 4736.

Source	RA(2000)	dec(2000)	Position error (")	Count rates ( $\times 10^{-3}$ count $s^{-1}$ )				Optical counterpart?
				SB	HB	HRIa	HRIb	
N4736-X1	$12^h 50^m 20.5^s$	$41^\circ 10' 03''$	13.9	-	$0.44 \pm 0.12$	-	-	-
N4736-X2	$12^h 50^m 23.2^s$	$41^\circ 07' 48''$	8.1	$1.71 \pm 0.26$	$1.45 \pm 0.17$	$1.20 \pm 0.14$	$1.00 \pm 0.24$	star? OR
N4736-X3	$12^h 50^m 28.5^s$	$41^\circ 13' 09''$	8.3	$1.38 \pm 0.25$	$0.76 \pm 0.15$	$0.58 \pm 0.11$	-	-
N4736-X4	$12^h 50^m 33.7^s$	$41^\circ 05' 07''$	14.8	-	$0.45 \pm 0.13$	-	-	OR
N4736-X5	$12^h 50^m 35.5^s$	$41^\circ 10' 19''$	12.0	-	$0.77 \pm 0.15$	-	-	OR
N4736-X6	$12^h 50^m 44.5^s$	$41^\circ 04' 49''$	8.3	-	-	$0.55 \pm 0.11$	-	OD
N4736-X7	$12^h 50^m 47.8^s$	$41^\circ 05' 03''$	8.4	-	$1.66 \pm 0.23$	$0.60 \pm 0.11$	-	OD
N4736-X8	$12^h 50^m 51.7^s$	$41^\circ 02' 48''$	11.2	-	$1.29 \pm 0.18$	-	-	OR
N4736-X9	$12^h 50^m 53.3^s$	$41^\circ 07' 07''$	8.0	$76.29 \pm 1.04$	$86.94 \pm 1.49$	$49.45 \pm 0.74$	$54.60 \pm 0.16$	nucleus
N4736-X10	$12^h 50^m 53.4^s$	$41^\circ 13' 08''$	13.6	-	$0.81 \pm 0.16$	-	-	-
N4736-X11	$12^h 50^m 59.6^s$	$41^\circ 02' 34''$	21.0	$1.05 \pm 0.25$	-	-	-	star? OR
N4736-X12	$12^h 51^m 00.0^s$	$41^\circ 11' 00''$	8.2	-	-	-	$1.74 \pm 0.32$	OR
N4736-X13	$12^h 51^m 03.7^s$	$41^\circ 07' 06''$	9.2	-	$1.05 \pm 0.16$	-	-	OD
N4736-X14	$12^h 51^m 05.7^s$	$41^\circ 09' 08''$	13.4	-	$0.43 \pm 0.13$	-	-	OD
N4736-X15	$12^h 51^m 15.8^s$	$41^\circ 06' 38''$	27.8	$0.98 \pm 0.24$	-	-	-	star(s)? OR

**Figure 1.** The discrete X-ray sources discovered in a  $12' \times 12'$  field centred on NGC 4736. The position of each source is marked by a circle with a radius equal to the positional uncertainty for that source. The X-ray data are shown superimposed on the DSS image of NGC 4736 with the ellipse marking the optical extent of the galaxy (see text).

## 4 X-RAY EMISSION FROM THE NUCLEAR SOURCE

### 4.1 Spatial properties

Source N4736-X9 in Table 2 is positionally coincident with the optical nucleus of the galaxy and is, by a substantial margin, the brightest X-ray source associated with the galaxy.

In the deep *ROSAT* PSPC observation in excess of 10000 counts were accumulated from this source; similarly 5000 counts were recorded in the HRIa observation. Thus these datasets allow a fairly detailed spatial analysis to be performed on, what we refer to hereafter as, the nuclear X-ray source in NGC 4736.

Inspection of both the *ROSAT* PSPC and HRI images

suggests that the X-ray emission from the nuclear source has a spatial extent well in excess of the predicted point spread function (PSF) for the two instruments. The magnitude of the effect was investigated by deriving the radial profiles of the X-ray emission. For this purpose the soft and hard band PSPC and HRIa data were rebinned onto a  $7.5'' \times 7.5''$  and  $4'' \times 4''$  pixel grid respectively. X-ray sources previously detected by PSS (other than the nuclear source itself) were then masked out, before calculating the radial profiles, centering in each case on the position of the peak surface brightness. The measured radial profiles are shown in Figure 2, which also for comparison shows the predicted PSF (the PSF was calculated from empirical formulae given by, Hasinger et al. (1995) for the PSPC and David et al. (1995) for the HRI). The nominal background was determined from source-excluded areas outside the region covered by the profile analysis.

Extended emission, surrounding the central nuclear source, is clearly seen in both PSPC bands and in the HRI data (Figure 2). This emission can be traced out to  $\sim 150''$  in all three cases and, in the case the PSPC soft band data, probably as far as  $\sim 200''$  before the signal merges with the background. At the distance of NGC 4736 the corresponding linear scales are approximately 3 and 4 kpc respectively. The total count rates are 0.138, 0.136 and 0.074 count  $s^{-1}$  for the soft and hard band PSPC and HRIa data respectively; the central point source contributes 55%, 64% and 66% of the signal in each channel. Since the signal from the HRI is predominately due to the hard band (0.5–2.0 keV) emission, the HRI result is consistent with the resolved fraction being  $\sim 10\%$  higher in the soft band.

The morphology of the extended emission in the nuclear region of NGC 4736 is illustrated by the contour plots in Figure 3, which are shown overlaid onto the DSS optical image of the galaxy. In each case the (fine-grid) images were smoothed by convolution with a two dimensional Gaussian (we used  $\sigma = 7.5''$  for the PSPC soft and hard bands and  $\sigma = 4''$  for the HRIa dataset). Figure 3 reveals some dissimilarity between the three cases. In the PSPC soft band there is evidence for a low surface brightness ridge of emission extending to the north of the nucleus (which, on the basis of the raw image could not be readily attributed to one or two faint point sources). This ridge gives rise to the apparent extension of the soft band radial profile in the  $150'' - 200''$  range. The central region of the soft band emission is fairly symmetric whereas in the hard band image there is a distortion caused by the presence of a relatively bright point source  $\sim 1'$  to the north-west of the galactic nucleus. This off-nucleus source contributes  $\sim 7.5\%$  of the total hard band counts\*. Potentially the contour map derived from the HRI data offers the best spatial resolution for studying the morphology of the extended emission of NGC 4736. In Figure 3(c) there is no evidence for the off-nucleus point source detected in the PSPC hard band image; however, a new point source is seen  $32''$  west of the nuclear source. This source contributes only  $\sim 2\%$  of the

total counts and is present at approximately the same count rate in the HRIb observation performed 18 days later. Overall the underlying extended emission seen in the HRI maintains a fairly symmetric form with just a hint of ellipticity in the contours along an east-west major axis.

Cui, Feldkhun & Braun (1997) in their earlier detailed analysis of the *ROSAT* PSPC data report the presence of the off-nucleus point source seen in the hard band image and also note the changed situation in the HRI (on the basis of a very preliminary look at the HRIb observation). They postulate that either the two sources are XRBs in the nuclear region of NGC 4736, or that the source is a foreground object crossing the line-of-sight to the galaxy with a high proper motion. The displacement between the X-ray source positions would imply a proper motion of  $\sim 8''$  per year, making the latter scenario highly improbable. The most likely explanation would seem to be that these are X-ray transients in the central region of NGC 4736. Based on the spectral form discussed earlier for XRBs we estimate the X-ray luminosity of the PSPC source to be  $\sim 3 \times 10^{38}$  erg  $s^{-1}$  (in agreement with Cui et al. 1997) whereas the HRI source has  $L_X \sim 9 \times 10^{37}$  erg  $s^{-1}$  (0.5–2.0 keV).

## 4.2 Spectral properties

The *ROSAT* PSPC and *ASCA* SIS and GIS instruments provide spectral coverage in the energy range 0.1–10 keV and together can be used to examine the broad band spectral characteristics of the nuclear source in NGC 4736. As a preliminary step, spectral fitting was performed on the *ASCA* SIS and GIS spectra in the restricted 2–10 keV range (throughout the spectral analysis the four spectra derived from the *ASCA* observation were fitted simultaneously using the same normalisation parameters). A spectral model consisting simply of a power-law continuum with line of sight absorption due to the Galactic hydrogen column density ( $N_H = 1.38 \times 10^{20}$  atoms  $cm^{-2}$ ; Stark et al. 1992), produced a reasonably good fit with a photon index  $\Gamma \sim 1.7$ . The replacement of the power-law with a bremsstrahlung continuum (with  $kT \sim 8$  keV) resulted in a similar match to the data. The inclusion of a narrow ( $\sigma = 50$  eV) Gaussian line component, to represent iron  $K_\alpha$  emission, led to a modest further improvement in the fit ( $\Delta\chi^2 \sim 7$ ). The best fit parameters (in the case of the power-law continuum) are listed in Table 3 as Model 1, where the errors correspond to 90% significance for one interesting parameter (see Yaqoob 1998). The line energy of  $\sim 6.8$  keV is consistent with the  $K_\alpha$  transition of He-like Fe (although the error range encompasses Fe XX – XXV, Makishima 1985) and the equivalent width is high,  $\sim 700$  eV, albeit with a large error (since this line is detected only at  $\sim 2.7\sigma$ ). When the power-law (or bremsstrahlung) model is extrapolated below 2 keV, the *ASCA* spectra reveal an excess of soft X-ray emission (Figure 4(a)). This soft excess flux may be satisfactorily modelled as emission from a solar abundance Raymond-Smith plasma (see Raymond & Smith 1977; Raymond 1992) with a temperature  $kT \sim 0.6$  keV (Model 2, Table 3).

As a final step in the spectral fitting the PSPC spectrum was also included in the analysis on the basis of the same spectral model as employed for the *ASCA* spectra (*i.e.* allowing no spectral or continuum variability in NGC 4736 between the two observation epochs). This demonstrated

\* The off-nucleus source was not detected by the PSS algorithm. This is almost certainly due to the use of a larger image pixel size in that analysis and the position of the source within the confines of the bright nuclear emission.

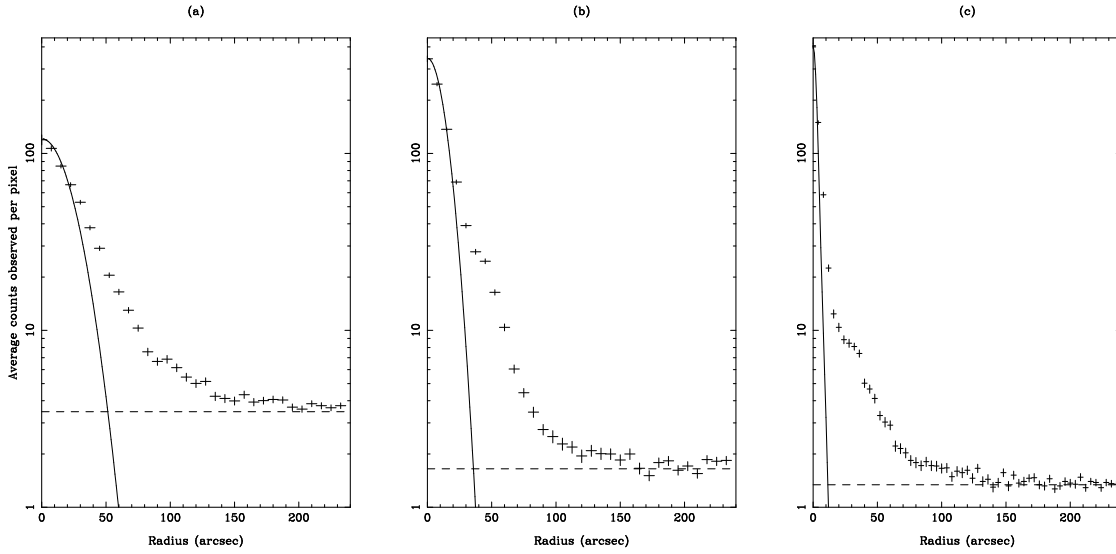


**Figure 2.** Radial profiles of the X-ray emission from the nuclear source in NGC 4736 as measured in (a) the PSPC soft band (b) the PSPC hard band and (c) the HRIa observation. The PSF for an on-axis source, normalised to the peak observed surface brightness, is shown as the solid line. The nominal detector background is indicated by the horizontal dashed line.

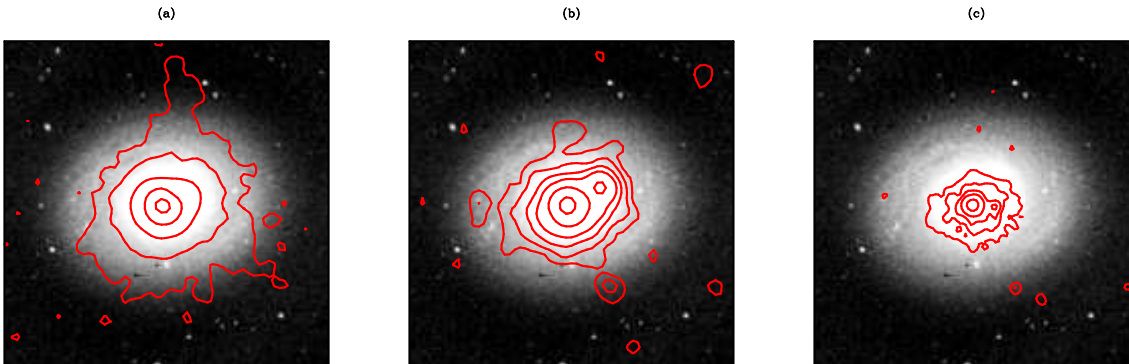


**Figure 3.** Contour maps of the extended X-ray emission region associated with the nuclear region of NGC 4736. The three panels correspond to (a) the PSPC soft band, (b) the PSPC hard band and (c) the HRIa observation. The contour levels are (a) 5, 10, 30, 65 and 100 count pixel<sup>-1</sup>; (b) 3, 5, 10, 20, 60 and 200 count pixel<sup>-1</sup>; and (c) 3, 6, 10, 20 and 100 count pixel<sup>-1</sup>. In each case the field of view is 8' × 8' and the contours are shown superimposed on the DSS optical image. The contour maps were smoothed by convolution with a two dimensional Gaussian, using  $\sigma = 7.5''$  for the PSPC soft and hard bands and  $\sigma = 4''$  for the HRIa dataset.

the need for a further (ultra-soft) spectral component (see Figure 4(a)), which we have modelled in terms of a second softer Raymond-Smith component. Again assuming a solar-abundance plasma we find that a temperature of  $kT \sim 0.1$  keV provides a good match to the spectral data. However, even after the addition of this new component to the spectral model, the  $\chi^2$  residuals in the fit suggested a considerable divergence between the *ASCA* and PSPC data in the 0.6–

1 keV range (Figure 4(b)). After various trials it was found that a greatly improved  $\chi^2$  could be achieved by the addition of a further narrow Gaussian line component at  $\sim 0.7$  keV, fitted only to the PSPC data (resulting in  $\Delta\chi^2 \sim 75$ ). The resulting fit parameters are given in Table 3 as Model 3 (see also Figure 4(c)). This line component may represent some form of contamination of the PSPC spectrum not removed in the background subtraction process (for example, Cui, Feld-

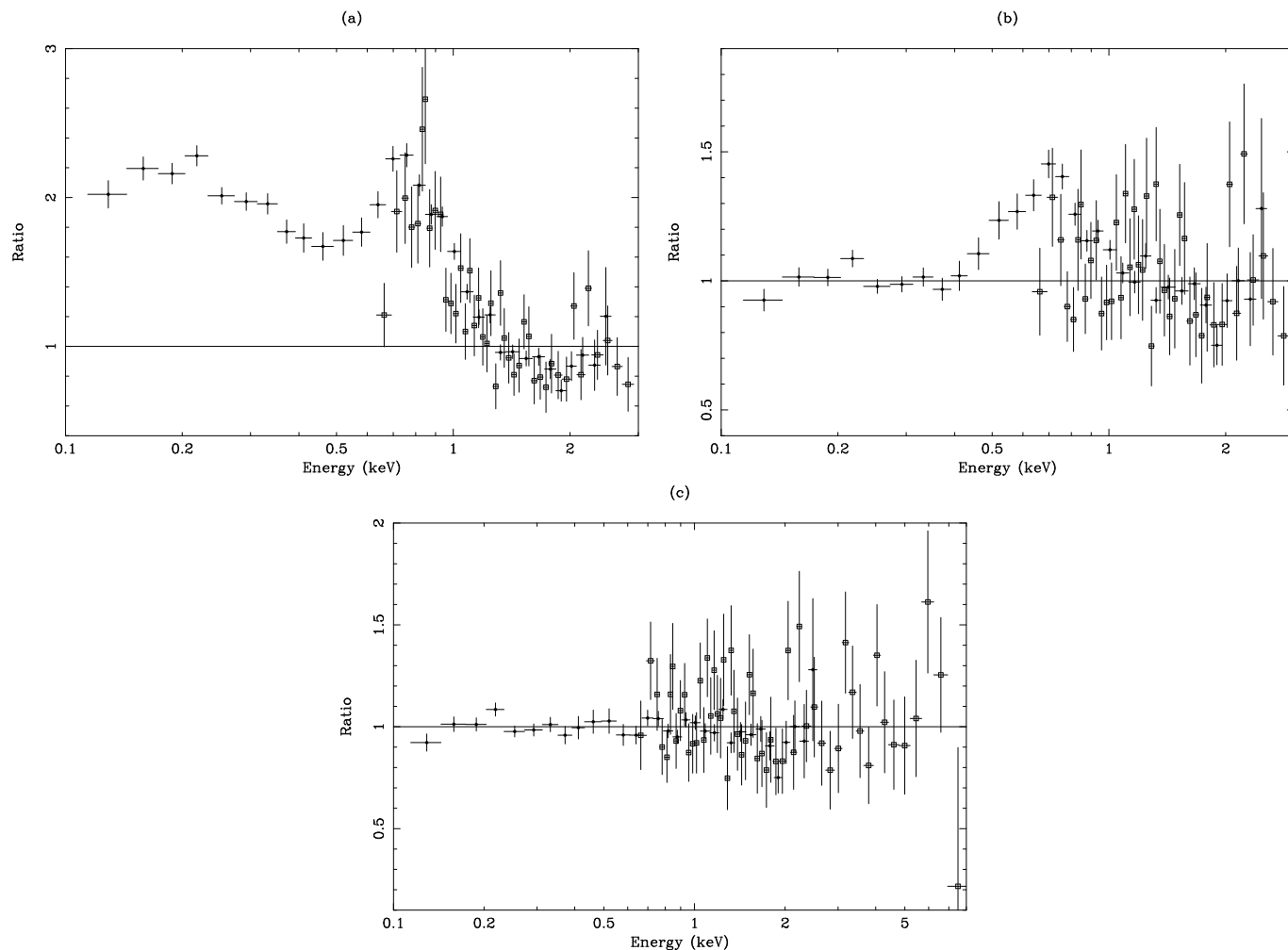


**Figure 4.** (a) The ratio of the *ASCA* (open squares) and *ROSAT* PSPC (solid dots) spectral data to the best-fitting Model-1 prediction, extrapolated into the 0.1–3 keV band. (b) The same ratio plot as in (a) but with the prediction based on Model 3 (except that here the equivalent width of the  $\sim 0.7$  keV Gaussian component is set to zero). (c) The same ratio plot as in (b) but with the 0.7 keV Gaussian component included. Note that this last plot covers a wider 0.1–8 keV spectral range. In all three cases only the *ASCA* SIS0 data are shown for clarity.

khun & Braun (1997) note that solar scattered X-rays are a particular problem in this PSPC observation) or alternatively may be a by-product (in terms of the spectral-fitting) of a cross-calibration error between *ROSAT* and *ASCA*.

The above spectral fitting analysis establishes that both a hard continuum component ( $\Gamma \sim 1.7$  or  $kT \sim 8$  keV) and softer thermal emission, characterised by temperatures in the range  $kT = 0.1 - 0.6$  keV, are present in the nuclear region of NGC 4736. Unfortunately, apart from the detection of the iron-line emission, there is insufficient signal to noise and spectral resolution to define the spectral characteristics in any greater detail. Thus, although we have assumed solar-abundance in the hot gas, equally good fits can be obtained if the abundance is dropped to 0.1 solar. Similarly it is not possible to constrain the line of sight column on the hard continuum (beyond the assumption of Galactic  $N_{\text{H}}$ ) since any intrinsic absorption is effectively masked by the soft thermal emission. The observations do confirm, however, that there was no very significant change in the level of the hard

component between the epochs of the *ROSAT* PSPC and *ASCA* observations<sup>†</sup>.

It is informative to examine the derived spectral model in relation to the spatial structure of the nuclear region established earlier. Hypothesizing that the extended emission is represented in the spectral model by the Raymond-Smith components, and the nuclear point source by the power-law continuum, then we predict, on the basis of the spectral model, that  $\sim 34\%$  of the photons in the 0.1–0.4 keV band and  $\sim 60\%$  in the 0.5–2 keV band are associated with the nuclear point source. By comparison the fractions determined from the spatial analysis are 55% and 64% (but with the possibility that the former is somewhat of an overestimate given the form of the radial distribution measured in the PSPC soft band, see Figure 2(a)). The implication is

<sup>†</sup> The off-nucleus transient source probably contributes  $\sim 10\%$  to the hard spectral emission detected in the PSPC observation; thus the flux comparison is reliable to no better than about 10%.

**Table 3.** The spectral fitting results for the nuclear source.

Parameter	Model 1	Model 2	Model 3
$N_{\text{H}_{fg}}^a$	1.38 <sup>f</sup>	1.38 <sup>f</sup>	1.38 <sup>f</sup>
$\Gamma_{PL}$	1.75±0.16	1.70±0.08	1.62 <sup>+0.07</sup> <sub>-0.08</sub>
$A_{PL}^b$	4.87 <sup>+0.98</sup> <sub>-0.83</sub>	4.44 <sup>+0.35</sup> <sub>-0.34</sub>	3.97 <sup>+0.26</sup> <sub>-0.25</sub>
$E_{K\alpha}^c$	6.81 <sup>+0.13</sup> <sub>-0.28</sub>	6.80 <sup>+0.13</sup> <sub>-0.28</sub>	6.80 <sup>+0.14</sup> <sub>-0.32</sub>
Eq. Width <sup>d</sup>	679 <sup>+414</sup> <sub>-412</sub>	661 <sup>+397</sup> <sub>-387</sub>	572 <sup>+378</sup> <sub>-357</sub>
$kT_{RS1}^c$	-	0.64 <sup>+0.05</sup> <sub>-0.06</sub>	0.65±0.05
$A_{RS1}^e$	-	1.09 <sup>+0.18</sup> <sub>-0.19</sub>	1.22±0.16
$kT_{RS2}^c$	-	-	0.10 ± 0.01
$A_{RS2}^e$	-	-	4.33 <sup>+0.34</sup> <sub>-0.41</sub>
$E_{\text{contam}}^c$	-	-	0.73 <sup>+0.02</sup> <sub>-0.03</sub>
Eq. Width <sup>d</sup>	-	-	481 <sup>+91</sup> <sub>-89</sub>
$\chi^2$	73.0	175.0	223.6
d.o.f.	66	163	191

<sup>a</sup>  $\times 10^{20}$  atoms  $\text{cm}^{-2}$ <sup>b</sup>  $\times 10^{-4}$  photon  $\text{cm}^{-2} \text{s}^{-1} \text{keV}^{-1}$ <sup>c</sup> keV<sup>d</sup> eV<sup>e</sup> XSPEC units<sup>f</sup> parameter value fixed

that the above division is at least plausible. Conversely, the presence of a bright point-source in the soft-band PSPC image argues against any significant intrinsic absorption of the hard continuum, although there is insufficient information to rule out more “contrived” spectral/spatial models.

### 4.3 Temporal properties

An analysis of all of the available observations reveals no evidence for any significant short-term temporal variability, over periods of tens of minutes to a few days, in the X-ray flux from the nuclear source in NGC 4736 (*c.f.* Cui et al. 1997). Also, as noted earlier, the spectral analysis is consistent with the level of the hard continuum component remaining unchanged between the *ROSAT* PSPC and *ASCA* observations, which were separated by a time interval of 4 years. A final check for temporal variability was possible by comparing the count rates measured for the unresolved central source in the spatial analysis of the hard-band PSPC data and the HR1a and HR1b observations. Specifically, assuming that this nuclear point source is the origin of the hard continuum identified in the spectral analysis, we have used the PIMMS package (Mukai 1996) to convert the measured count-rates into fluxes. The count rates associated with the point source in the three cases convert to 0.5–2 keV fluxes of  $\sim 1.0, 1.2$  and  $1.3 \times 10^{-12} \text{ erg cm}^{-2} \text{ s}^{-1}$  respectively. Any long term variability implied by these measurements is therefore at an amplitude  $\lesssim 30\%$ .

## 5 DISCUSSION

X-ray observations can, in principle, provide crucial information relating to the question of whether galaxies classified as LINERS generally harbour LLAGN at their centres. In the case of NGC 4736, our analysis of the X-ray emission from its nuclear region confirms the presence of a bright X-ray point source coincident with the optical nucleus. We associate this compact source with the hard continuum evident in the 2–10 keV band. Modelled as a power-law, the luminosity of this hard continuum is  $\sim 2 \times 10^{39} \text{ erg s}^{-1}$  in the 0.5–2 keV band, and  $\sim 4 \times 10^{39} \text{ erg s}^{-1}$  in the 2–10 keV range. The measured slope of the power-law corresponds to a photon spectral index  $\Gamma \sim 1.7$ , which is fairly typical of Seyfert 1 galaxies in the 2–10 keV band (e.g. Turner & Pounds 1989; Nandra & Pounds 1994). Thus, taking into account the lack of any clear signature of continuum absorption, a possible interpretation of the NGC 4736 X-ray spectrum is that in the X-ray regime we have a direct view of a LLAGN which, apparently, is in a near quiescent state (in that the observed luminosity is a factor  $10^3 - 10^6$  lower than is typically of Seyfert nuclei). The existence of active galactic nuclei with very low X-ray luminosities is now well established (e.g. M 81, Ishisaki et al. 1996; NGC 4258, Makashima et al. 1994; NGC 3147, Ptak et al. 1996; M51 Terashima et al. 1998a) and in the most extreme case reported to date, namely that of NGC 4395, the dwarf Seyfert nucleus was found to have an  $L_X$  of only  $\sim 3 \times 10^{38} \text{ erg s}^{-1}$  (Lira et al. 1998).

In order to confirm the supposition that the LINER nucleus in NGC 4736 contains a LLAGN it is necessary to consider what further clues are provided by the X-ray data. Support for the presence of a LLAGN could in principle come from the observation of significant continuum variability. If LLAGN are the direct low-luminosity analogue of the classical Seyfert phenomenon then the trend of increasing variability with decreasing luminosity displayed in Seyfert galaxies (Nandra et al. 1997a) would predict LLAGN to be highly variable X-ray sources. This property is not apparent in the sample of LLAGN and LINERs studied by Ptak et al. (1998), although M 81 and NGC 4395 do vary on a timescale of  $\sim$  weeks. Ptak et al. (1998) argue that since LLAGN must be accreting at grossly sub-Eddington rates, they are likely to be powered by an advection-dominated accretion flow (Narayan & Yi 1995), a scenario in which rapid X-ray variability can be suppressed. In any event, it is not possible to use the absence of X-ray temporal variability in NGC 4736 on timescales of  $\sim$  hours to days as a strong argument either for or against the LLAGN hypothesis.

Potentially the most important clue we have as to the origin of the hard X-ray emission is provided by the detection of the Fe  $K_\alpha$  emission line, with recent results from *ASCA* amply demonstrating the diagnostic possibilities of such features (*e.g.* Nandra et al. 1997a). In the case of NGC 4736 we detect (albeit at marginal significance) a Fe-K line with a high equivalent width ( $\sim 600 \text{ eV}$ ) at an energy inconsistent with the fluorescence in cold gas. The most obvious explanation of the large equivalent width, by analogy to the situation pertaining in classical Seyfert 2 galaxies such as NGC 1068 (see Antonucci 1993), is that the direct line-of-sight to the central engine is completely blocked, perhaps by a molecular torus, but nevertheless we see a fraction of the nuclear flux as a result of electron scattering. This scattering



occurs in a photoionised medium which extends sufficiently far from the nucleus, probably along an axial direction, so as to be visible above the plane of the obscuring medium. Typically up to a few percent of the nuclear continuum can be redirected into our line of sight and a substantial Fe-K line feature is superimposed due to the fluorescence of the scattering medium. Iron line equivalent widths greater than 1 keV can be produced by this means (*e.g.* Makashima 1985), with the line energy providing a measure of the ionisation state of the electron scattering region. For example, at least two *high energy* Fe-K components are detected with high equivalent width in the X-ray spectrum of NGC 1068, indicative of the presence of a warm scattering medium (Marshall et al. 1993; Ueno et al. 1994; Iwasawa, Fabian & Matt 1997).

In the case of NGC 4736, the combination of the observed Fe-K feature, the absence of temporal variability and the lack of any clear signature of continuum absorption constitute circumstantial evidence in favour of a scattering scenario (with the implication that the direct nuclear emission is blocked by a column density well in excess of  $10^{24}$  cm<sup>-2</sup>). The luminosity of the “hidden” LLAGN might then be close to  $10^{41}$  erg s<sup>-1</sup> (if we assume a scattered fraction of roughly 3% of the total nuclear continuum). A test of whether NGC 4736 might harbour such an “unseen” type-2 nucleus is provided by reference to its far-infrared flux. David et al. (1992) derive a linear relationship between the FIR luminosity (based on 60 and 100 micron fluxes) and the (0.5–4.5 keV) X-ray luminosities of a sample of normal, starburst and LINER galaxies. Applied to NGC 4736, the David et al. formula predicts an expected X-ray luminosity of  $\sim 5 \times 10^{39}$  erg s<sup>-1</sup> in close agreement to that actually observed. In principle this argues against *any* LLAGN presence in NGC 4736, but given the scatter in the David et al. correlation, it remains a reasonable conjecture that a LLAGN at a “quiescent” level of a few times  $10^{39}$  erg s<sup>-1</sup> has escaped detection in other wavebands. However, the requirements for a much more luminous hidden LLAGN look implausible. Similarly the observed  $L_{[\text{OIII}]}/L_X$  ratio for NGC 4736 is much closer to the norm for unobscured Seyfert nuclei than for galaxies with hidden Seyfert nuclei such as NGC 1068 (Mulchaey et al. 1994). Unfortunately in the quiescent LLAGN scenario we are left with the problem of how to explain both the observed energy and equivalent width of the Fe K $_{\alpha}$  line. Terashima et al. 1998b discuss the relevant arguments in the context of the LINER galaxy NGC 4579, which also has a strong He-like iron Fe-K line in its *ASCA* spectrum.

There is of course an alternative to the LLAGN hypothesis, namely that all of X-ray flux emanating from nuclear point source in NGC 4736 is generated by stellar mass objects in the nucleus of the galaxy. Given the relatively hard spectrum, the most likely population would seem to be low and/or high mass X-ray binaries (XRB) (see Fabbiano 1989; Makishima et al. 1989). For example,  $\lesssim 40$  XRB concentrated in the nucleus of the galaxy, powered at near to their Eddington limit by accretion onto a neutron star or stellar mass black-hole, could produce both the observed X-ray luminosity and the hard spectral form. Also in this model, since the observed X-ray flux is due to the integrated emission of a reasonable number of separate sources, a substantial amplitude of variability is not expected. The one major

difficulty with this description is in explaining the apparently large equivalent width of the Fe K line in NGC 4736, since individual XRB tend to have Fe K lines with equivalent widths of only a few tens of eV (Hirano et al. 1987), which is well outside the formal 90% confidence range of the measurement. As a check of the XRB model we can utilize the fact that, in the absence of an AGN, the optical luminosity of a spiral galaxy bulge is often well correlated with its X-ray luminosity due to its population of XRBs (Canizares, Fabbiano & Trinchieri 1987). In the case of NGC 4736 this method predicts, on the basis of the optical magnitude of the bulge of NGC 4736 ( $M_B = -18.19$ ; Ho, Filippenko & Sargent 1997) and Figure 5 of Iyomoto et al. (1998), an X-ray luminosity of  $\sim 1 \times 10^{39}$  erg s<sup>-1</sup>, which is a factor four below that observed. However, an over-density of XRBs, particularly in a region characterised by recent intense starburst activity, perhaps with an XRB population biased toward high mass systems, cannot be excluded,

An interesting feature of bright nuclear X-ray source in NGC 4736 is that over a third of the X-ray emission below 2 keV is resolved with a radial extent of  $\sim 150''$ , *i.e.*  $\sim 3$  kpc. We associate this extended emission with the two thermal components identified in the spectral analysis with temperatures of 0.1 and 0.65 keV, which have a combined luminosity of  $\sim 2 \times 10^{39}$  erg s<sup>-1</sup> in the 0.1–2 keV PSPC band. The observed thermal emission is largely confined within the bright circumnuclear ring of star-forming regions identified in H $\alpha$  and other wavebands. A possible origin of this hot gas is in a starburst event (or events) which have occurred in the nucleus of NGC 4736. Hydrodynamic modelling of starbursts (*e.g.* Suchkov et al. 1994; Tenerio-Tagle & Muñoz-Tuñón 1997) has been broadly successful in duplicating the results of X-ray observations that show kpc scale “plumes” of hot X-ray emitting gas escaping from the disc into the halo of galaxies experiencing nuclear starbursts (*e.g.* NGC 253, Pietsch & Trümper 1993). For the hotter plasma observed we derive a volume emissivity of  $\sim 2 \times 10^{-27}$  erg cm<sup>-3</sup> s<sup>-1</sup> (assuming spherical symmetry and a concentration of the emission within a radius of  $100''$ ), an electron density of  $\sim 10^{-2}$  cm<sup>-3</sup> and a cooling time of  $\sim 10^9$  yr (Tucker 1975). Hence the hot extended plasma component may indeed have had its origin in a recent starburst epoch.

Unfortunately, the modelling of the soft X-ray excess observed in NGC 4736 in terms of two specific temperature components may not represent an accurate picture of the state of the hot plasma in this galaxy. A variety of effects such as a departure from non solar-abundances, a smooth spread of temperature values and non-equilibrium conditions in the plasma may have combined to mimic a two-temperature spectrum (given the limited spectral resolution and sensitivity afford by the combined *ROSAT* and *ASCA* data). Equally well it is possible to hypothesize that the two Raymond-Smith components may represent two distinct spatial distributions, for example the hotter plasma could be located within the disc of the galaxy with the cooler component forming a more diffuse halo. Unfortunately, the only real evidence for such a spatial segregation is given by the low-surface brightness North-South ridge of emission, evident in the soft band but not the hard band PSPC image.

## 6 CONCLUSION

There has been considerable recent interest in the identification of candidate LLAGN in the nuclei of nearby galaxies via X-ray measurements. From *ASCA* observations we know that many of the sources established as bona-fide LLAGN have broadly similar spectral characteristics to those observed in the nuclear source in NGC 4736, namely a hard continuum, a detectable Fe-K line and a softer, probably thermal component, which is prominent below 2 keV (see Serlemitsos, Ptak & Yaqoob 1996). Unfortunately, despite this apparent conformity, we are still unable to answer the key question of whether the LINER nucleus in NGC 4736 contains an X-ray bright LLAGN with complete certainty. Fortunately, we can be fairly sure that when high sensitivity X-ray observations with good spectral and spatial resolution become available from *AXAF* and *XMM*, a definitive answer will be forthcoming. As in many areas of X-ray astrophysics, the Fe-K line may well provide the crucial diagnostic.

## 7 ACKNOWLEDGEMENTS

TPR acknowledges support from PPARC initially in the form of a research studentship and more recently as a post-doctoral research associate. The X-ray spectral data used in this work were obtained from the Leicester Data Archive Centre (LEDAS) and the HEASARC facility at Goddard Space Flight Centre, USA. The Digitized Sky Survey was produced at the Space Telescope Science Institute, under US Government grant NAG W-2166 from the original National Geographic - Palomar Sky Survey Plates.

## REFERENCES

- Allan, D.J. *Asterix user note 004*. CCLRC/Rutherford Appleton Laboratories, 1995
- Antonucci, R., 1993, *ARA&A*, 31, 473
- Bosma, A., van der Hulst, J.M., Sullivan, W.T., 1977, *A&A*, 57, 373
- Brandt, W.N., Pounds, K.A., Fink, H., 1995, *MNRAS*, 273, 47
- Buta, R., 1988, *ApJS*, 66, 233
- Canizares, C.R., Fabbiano, G., Trinchieri, G., 1987, *ApJ*, 312, 503
- Cui, W., Feldkhun, D., Braun, R., 1997, *ApJ*, 477, 693
- David, L.P., Harnden, F.R., Kearns, K.E., Zombeck M.V. *The ROSAT High Resolution Imager (HRI)*, US *ROSAT* Science Data Center/SAO, 1995
- David, L.P., Jones, C., Forman, W., 1992, *ApJ*, 388, 82
- Fabbiano, G., 1989, *ARA&A*, 27, 87
- Filippenko, A.V., Sargent, W.L.W., 1985, *ApJS*, 57, 503
- Gerin, M., Casoli, F., Combes, F., 1991, *A&A*, 251, 32
- Hasinger, G., Burg, R., Giacconi, R., Hartner, G., Schmidt, M., Trümper, J., Zamorani, G., 1994, *A&A*, 291, 348
- Hasinger, G., Turner, T.J., George, I.M., Boese, G., *The On-Axis Point Spread Function: In-flight comparison with the PANTER results*. OGIP Calibration Memo CAL/ROS/92-001, 1995
- Heckman, T.M., Balick, B., Crane, P.C., 1980, *A&AS*, 40, 295
- Hirano, T., Hayakawa, S., Nagase, F., Masai, K., Mitsuda, K., 1987, *PASJ*, 39, 619
- Ho, L.C., Filippenko, A.V., Sargent, W.L.W., 1998, *in prep.*
- Ho, L.C., Filippenko, A.V., Sargent, W.L.W., 1997, *ApJS*, 112, 315
- Ishisaki, Y., Makashima, K., Iyomoto, N., Hayashida, K., Inoue, H., Mitsuda, K., Tanaka, Y., Uno, S. Kohmura, Y., Mushotzky, R.F., Petre, R., Serlemitsos, P.J., Terashima Y., 1996, *PASJ*, 48, 237
- Iwasawa, K., Fabian, A.C., Matt, G., 1997, *MNRAS*, 289, 433
- Iyomoto, N., Makashima, K., Matsushita, K., Fukazawa, Y., Tashiro, M., Ohashi, T., 1998, *preprint*
- Larkin, J.E., Armus, L., Knop, R.A., Soifer, B.T., Matthews, K., 1998, *ApJS*, 114, 59
- Lira, P., Lawrence, A., O'Brien, P., Johnson, R., Terlevich, R., Bannister, N., 1998, *MNRAS*, *submitted*
- Makashima, K., Fujimoto, R., Ishisaki, Y., Kii, T., Loewenstein, M., Mushotzky, R., Serlemitsos, P., Sonobe, T., Tashiro, M., Yaqoob, T., 1994, *PASJ*, 46, 77
- Makashima, K., 1985. In: *The physics of accretion onto compact objects*, K.O. Mason and M.G. Watson and N.E. White, eds., Springer-Verlag, p. 249.
- Makashima, K., Ohashi, T., Hayashida, K., Inoue, H., Koyama, K., Takano, S., Tanaka, Y., Yoshida, A., Turner, M.J.L., Thomas, H.D., Stewart, G.C., Williams, R.O., Awaki, H., Tawara, Y., 1989, *PASJ*, 41, 697
- Maoz, D., Filippenko, A.V., Ho, L.C., Rix, H.-W., Bahcall, J.N. Schneider, D.P., Macchetto, F.D., 1995, *ApJ*, 440, 91
- Marshall, F.E., Netzer, H., Arnaud, K.A., Boldt, E.A., Holt, S.S., Jahoda, K.M., Kelley, R., Mushotzky, R.F., Petre, R., Serlemitsos, P.J., Smale, A.P., Swank, J.H., Szymkowiak, A.E., Weaver, K.A., 1993, *ApJ*, 405, 168
- Möllenhoff, C., Matthias, M., Gerhard, O.E., 1995, *A&A*, 301, 359
- Mukai, K., *PIMMS version 2.3 Users Guide*, 1996
- Mulchaey, J.S., Koratkar, A., Ward, M.J., Wilson, A.S., Whittle, M., Antonucci, R.R.A., Kinney, A.L., Hurt, T., 1994, *ApJ*, 436, 586
- Mulder, P.S., van Driel, W., 1993, *A&A*, 272, 63
- Nandra, K., George, I. M., Mushotzky, R. F., Turner, T. J., Yaqoob, T., 1997a, *ApJ*, 476, 70
- Nandra, K., George, I.M., Mushotzky, R.F., Turner, T.J., Yaqoob, T., 1997b, *ApJ*, 477, 602

- Nandra, K., Pounds, K.A., 1994, MNRAS, 268, 405  
Narayan, R., Yi, I., 1995, ApJ, 452, 710  
Pietsch W., Trümper, J., 1993, AdSpR, 13, 171  
Pogge, R.W., 1989, ApJS, 71, 433  
Ptak, A., Yaqoob, T., Mushotzky, R., Serlemitsos, P., Griffiths, R., 1998, ApJL, 501, 37  
Ptak, A., Yaqoob, T., Serlemitsos, P.J., Kuneida H., Terashima, Y., 1996, ApJ, 459, 542  
Raymond, J.C., Smith, B.W., 1977, ApJS, 35, 419  
Raymond, J.C., 1992, ApJ, 384, 502  
Read, A.M., Ponman, T.J., Strickland, D.K., 1997, MNRAS, 286, 626  
Serlemitsos, P., Ptak, A., Yaqoob, T., 1996. In: *The physics of LINERS in view of recent observations*, Eracleous, M., Kotorakar, A., Leitherer, C., Ho, L., eds., p. 70  
Singh, K.P., Barrett, P., White, N.E., Giommi, P., Angelini, A., 1995, ApJ, 455, 456  
Smith, B.J., Lester, D.F., Harvey, P.M., Pogge, R.W., 1991, ApJ, 373, 66  
Smith, B.J., Harvey, P.M., Colomé, C., Zhang, C.Y., DiFrancesco, J., Pogge R.W., 1994, ApJ, 425, 91  
Stark, A., Gammie, C.F., Wilson, R.W., Bally, J., Linke, R.A., Heiles, C., Hurwitz, M., 1992, ApJS, 79, 77  
Struck, C., Appleton, P.N., Borne, K.D., Lucas, R.A., 1996, AJ, 112, 1868  
Suchkov, A., Balsara, D., Heckman, T., Leitherer, C., 1994, ApJ, 430, 511  
Taniguchi, Y., Wada, K., 1996, ApJ, 469, 581  
Taniguchi, Y., Ohshima, Y., Yameda, T., Mouti, H., Yoshida, M., 1996, ApJ, 467, 215  
Tenerio-Tagle, G., Muñoz-Tuñón, C., 1997, ApJ, 478, 134  
Terashima, Y., Ptak, A., Fujimoto, R., Itoh, M., Kuneida, H., Makashima, K., Serlemitsos, P.J., 1998a, ApJ, 496, 210  
Terashima, Y., Kuneida, H., Misaki, K., Mushotzky, R.F., Ptak, A., Reichert, G.A., 1998b, ApJ, *in press*  
Tucker, W.H., 1975, *Radiation Processes in Astrophysics*, MIT Press.  
Tully, R.B., 1988, *Nearby Galaxies Catalog*, Cambridge University Press  
Turner, J.L., Ho, P.T.P., 1994, ApJ, 421, 122  
Turner, T.J., Pounds, K.A., 1989, MNRAS, 240, 833  
Ueno, S., Mushotzky, R.F., Koyama, K., Iwasawa, K., Awaki, H., Hayashi, I., 1994, PASJ, 46, 71  
van den Heuvel, E.D.F., Bhattacharya, D., Nomoto, K., Rappaport, S.A., 1992, A&A, 262, 97  
Yaqoob, T., 1998, ApJ, 500, 893